

Low cost integration of 3D-electrodes via replica molding

Benjamin Mustin and Boris Stoeber

The University of British Columbia, Canada

ABSTRACT

We demonstrate a new replica molding method for integrating 3D-composite electrodes into microfluidic devices made from polydimethylsiloxane (PDMS) at low cost. Our process does not require work in a cleanroom, expensive materials, or expensive equipment once a micro mold has been fabricated using standard multilayer SU-8 photolithography. Different device geometries have been fabricated to demonstrate the capabilities and limitations of the method. The electrical properties of the composite electrode material are characterized. Furthermore, a device for concentrating particles via AC-dielectrophoresis (DEP) is presented as an example for a potential application of the fabrication process.

KEYWORDS: replica molding, electrodes, electrokinetics, particles, PDMS composite

INTRODUCTION

Methods for integrating microscopic conductive features into microfluidic devices are of great importance for the lab-on-a-chip community [1]. These features can serve as electrodes for the generation of electric fields, with applications including sample concentration, sample separation, electrochemical measurements, mixing, electroporation and electro-fusion of cells. Despite their importance, most methods for integrating conductive features into microfluidic devices require either expensive materials, equipment or photolithography steps for each device to be fabricated. Although the integration of electrodes via injection molding methods [2] have fewer requirements, the range of the achievable electrode geometries is rather limited. This work presents an affordable replica molding method that allows integrating a large variety of conductive features into microfluidic devices.

THEORY

Micromold masters required for fabricating microfluidic devices with integrated 3D electrode structures by replica molding are produced in a cleanroom using standard multilayer SU-8 (MicroChem) photolithography. Copies of the mold masters can be fabricated from polyurethane (Smooth cast 310, Smooth-on) using the process described in [3]; the replica molding procedure illustrated in Figure 1 is then performed using these copies or the original master. Throughout the process, the PDMS (Sylgard 182, Dow Corning) is used in a 10:1 (base:hardener) ratio.

The method presented here is based on a dry nanoparticle embedding technique that was recently demonstrated for fabricating magnetic polymer micropillars for MEMS applications [4]. Carbon black (CB) nanoparticles (Vulcan XC72R, Cabot) are applied to the mold in dry form using a tongue depressor. A crucial step is the removal of the excess particles by casting them into PDMS as shown Figure 1c. The micromolds incorporate barriers surrounding the main features as shown in Figure 1(h). These barriers facilitate the casting process as controlled volumes of uncured PDMS can be applied to the mold using a micropipette until the PDMS film fills the whole area within the barrier as shown in Figure 1(i) for a clean wafer.

Electrical chip to world connections are made by punching holes into the PDMS device in regions 4 and 5 (Figure 1h). These regions are filled with CB-PDMS composite connecting to the electrodes in the microfluidic channels. After the PDMS has been bonded to a glass slide by oxygen plasma bonding, the punched holes are filled with a CB-PDMS composite. Stranded wires are then inserted into the holes filled with CB-PDMS composite and the device is cured in an oven.

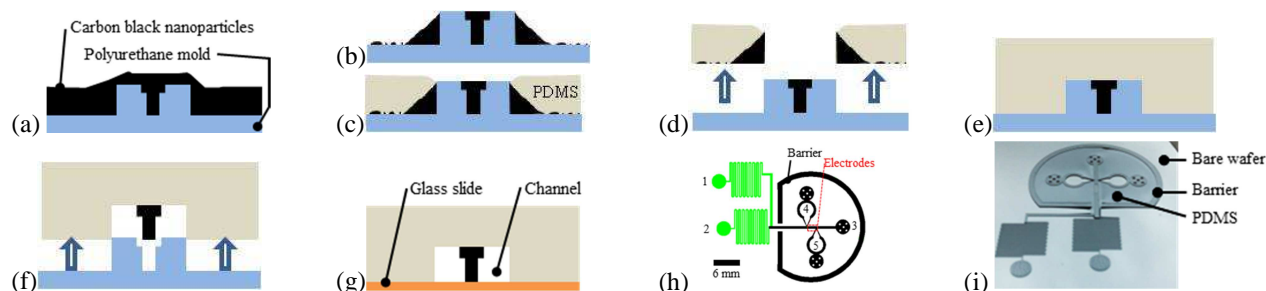


Figure 1: Process overview: (a) Application of CB particles to the mold using a tongue depressor. (b) Removal of excess particles using a cotton applicator. (c) Casting of the remaining excess particles into PDMS. (d) Curing and removal of the thin layer of PDMS. (e) Covering of the mold with PDMS and curing at room temperature overnight. (f) Peeling of the PDMS. (g) Bonding of the PDMS to a glass slide or to another fluidic layer seals the channel. (h) General device layout: 1, 2 and 3 are fluidic inlet and outlet ports; 4 and 5 indicate the locations for the electrical chip-to-world connections. (i) Silicon substrate with SU-8 mold structures after the application of PDMS with a pipette to remove the excess CB.

EXPERIMENTAL

Devices following the layout shown in Figure 1(h) were fabricated with different electrode geometries in order to demonstrate the capabilities of the fabrication method. A complete device and different electrode geometries are shown in Figure 2.

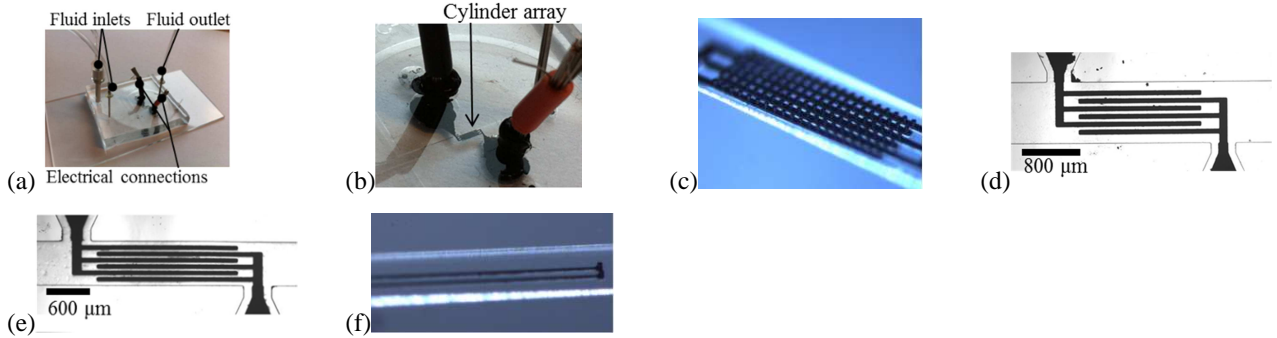


Figure 2: (a) and (b) Image of a device containing an array of conductive cylinders (black) with a diameter of $40\ \mu\text{m}$ and a height of $45\ \mu\text{m}$ connected to leads with a $60\ \mu\text{m} \times 35\ \mu\text{m}$ cross section in an $800\ \mu\text{m}$ wide and $80\ \mu\text{m}$ high channel as shown in (c). (d) and (e) top-view of the cylinder array with (d) $40\ \mu\text{m}$ and (e) $20\ \mu\text{m}$ gaps between the leads. (f) Cylinders with the same dimensions as in (c) connected to $20\ \mu\text{m} \times 20\ \mu\text{m}$ leads.

For the characterization of the electrical properties of the CB-PDMS composite, devices consisting of leads of 1 cm length with a cross section of $100\ \mu\text{m} \times 93\ \mu\text{m}$ were fabricated using the procedure described in Figure 1(a)-(f). The conductivity of the CB-PDMS composite and the resistance of the electrical chip to world connections were determined in 4-point measurements. Additionally, two-point impedance measurements were performed using a 4294A Precision Impedance Analyzer (Agilent) in the shielded four-terminal (4T) configuration.

In order to demonstrate a potential application for the fabrication process, a device for the concentration of polystyrene particles via AC-DEP was designed and tested. The devices incorporate an array of cylinders connected to leads as shown in Figure 2(c) and (d). The performance of the device was evaluated experimentally by determining the flux J_{dep} of trapped particles using the setup shown in Figure 3(a). The electrodes are connected to a function generator that produces a sinusoidal voltage signal and a voltage amplifier. During an experiment a suspension of fluorescent polystyrene (PS) particles (Thermo Scientific) with a mean diameter of $d = 1\ \mu\text{m}$ and with the volume concentration of particles of $C_{\text{in}} = 0.0075\ \text{vol}\%$ was driven through the device at a flow rate Q using a syringe pump. The concentration of the particles downstream from the post array C_{out} was measured using fluorescence microscopy while particles were accumulating in the concentration region. Assuming that the particle concentration is uniform over the depth of the channel and that the fluid velocity is uniform, the approximate average downstream particle flux was calculated from

$$J_{x\text{-out}}(t_k) = \frac{Q A_{\text{px}}}{\Delta x_{\text{FOV}} W} \sum_i \sum_j C_{\text{out}}(x_i, y_j, t_k), \quad (1)$$

where $\Delta x_{\text{FOV}} = 1\ \text{mm}$ is the length of the field of view (FOV), W is the channel width and A_{px} is the area of one pixel (the summation is performed over the FOV). The particle trapping rate $J_{\text{dep}}(t)$ was then calculated from the difference between incoming particle flux and outgoing particle flux.

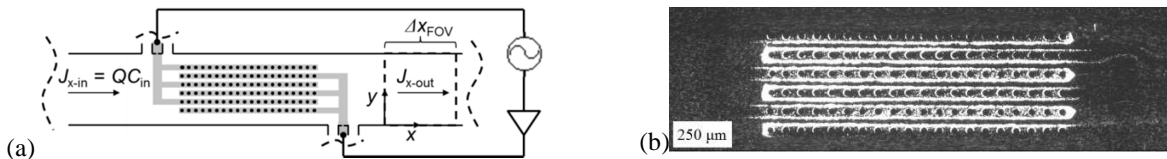


Figure 3: (a) Experimental setup for particle concentration experiments. (b) Microscopic image of particles (appear bright) accumulating in regions of high field intensity.

RESULTS AND DISCUSSION

As shown in Figure 2, a great variety of electrode geometries can be realized with the fabrication process described above.

The mean conductivity and the corresponding standard deviation determined from 33 lead resistance measurements was $16.74\ \text{S/m}$ and $8.1\ \text{S/m}$ respectively. The mean and the standard deviation of the contact resistance determined from six measurements were $2.44\ \text{k}\Omega$ and $1.61\ \text{k}\Omega$ respectively. Impedance data for three samples with lead resistances ranging from close to the mean resistance (Sample 1) to close to the maximum measured resistance (Sample 3) are shown in Figure 4. The magnitude of the impedance was normalized with respect to the magnitude of the impedance at $f = 40\ \text{Hz}$ where $|Z|_{40\text{Hz}} =$

73 k Ω , 109 k Ω and 244 k Ω for sample 1, 2 and 3, respectively. All samples show resistive behavior for frequencies below 1 MHz, which makes the CB-PDMS composite suitable for AC-electrokinetic applications such as particle concentration via AC-DEP.

Particle trapping rates obtained from the setup described in the preceding section are shown in Figure 5a. The trapping rates decrease over time while particles accumulate at the electrodes. The initial (maximum) deposition rate J_{dep}^0 is independent of frequency in the investigated range as shown in Fig 5b. Further, the initial rate J_{dep}^0 is found to be governed by convection and dielectrophoresis; the quadratic increase of J_{dep}^0 with the applied voltage for $U_{\text{rms}} < 10\text{V}$ in Fig 5c indicates that dielectrophoresis is the rate limiting factor. At higher voltages, convection seems rate limiting through particle depletion as indicated by the linear increase of J_{dep}^0 with the flow rate in Fig 5d.



Figure 4: Impedance data for three samples with different CB-PDMS lead resistances: (a) Normalized magnitude of the impedance. (b) Phase data

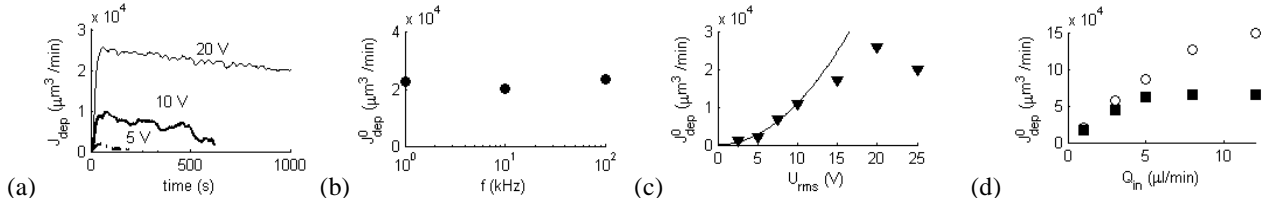


Figure 5: (a) Deposition rates for different applied potentials U_{rms} at $Q = 1\mu\text{l}/\text{min}$, $C_{\text{in}} = 0.0075\% \text{wt}$ and $f = 100\text{kHz}$. (b) Initial deposition rate at $Q = 1\mu\text{l}/\text{min}$ for three frequencies and (c) for different input voltages U_{rms} at $f = 100\text{kHz}$. The solid line represents the fit $J_{\text{dep}}^0 = a(U_{\text{rms}})^2$ with $a = 109.9\mu\text{m}^3/\text{min}/\text{V}^2$. (d) Initial deposition rate as a function of flow rate for the two input voltages $U_{\text{rms}} = 15\text{V}$ (squares) and $U_{\text{rms}} = 25\text{V}$ (circles) at $f = 100\text{kHz}$.

CONCLUSIONS

A method for integrating 3D-electrode structures into microfluidic devices made from polydimethylsiloxane was demonstrated. The method has several advantages over previous methods. It is comparably affordable and does not rely on expensive equipment once a micromold master has been fabricated. Great flexibility in achievable electrode geometries was demonstrated. No aligning between an electrode layer and a fluidic layer is required and the devices are leakage free. Particles made from materials with higher bulk conductivity could be used in case a higher conductor conductivity is required. The fabrication process yields devices that are suitable for electrokinetic applications as demonstrated with a device for the concentration of PS particles via AC-DEP.

ACKNOWLEDGEMENTS

This work was supported by the Natural Science and Engineering Research Council (NSERC) of Canada through the Special Research Opportunity program.

REFERENCES

- [1] S. Haeberle, and R. Zengerle, Microfluidic platforms for lab-on-a-chip applications Lab on a Chip, Royal Society of Chemistry, vol. 7, pp. 1094-1110 (2007)
- [2] A. Pavesi, F. Piraino, G. B. Fiore, K. M. Farino, M. Moretti, and M. Rasponi, How to embed three-dimensional flexible electrodes in microfluidic devices for cell culture applications, Lab on a Chip, vol. 11, pp. 1593-1595 (2011)
- [3] S. P. Desai, D. M. Freeman, and J. Voldman, Plastic masters-rigid templates for soft lithography, Lab on a Chip, Royal Society of Chemistry, vol. 9, pp. 1631-1637 (2009)
- [4] F. Khademolhosseini, and M. Chiao, A dry nanoparticle embedding technique for fabrication of magnetic polymer micropillars, Proc 2012 IEEE 25th International Conference on MEMS, pp. 212 -215 (2012)

CONTACT

Benjamin Mustin, +1 604 827 4593, mustin@mech.ubc.ca